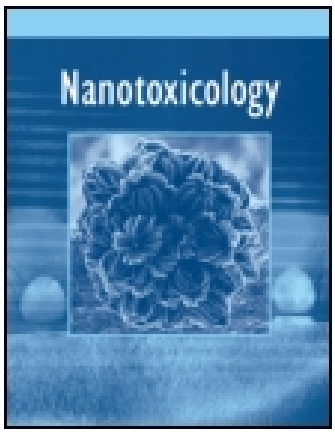

Nanotoxicology
Publication details, including instructions for authors and subscription information:
http://www.tandfonline.com/loi/inan20

Toxicity screenings of nanomaterials: challenges due to interference with assay processes and components of classic in vitro tests

Rina Guadagnini[a], Blanka Halamoda Kenzaoui[b], Laura Walker[c], Giulio Pojana[df], Zuzana Magdolenova[e], Dagmar Bilanicova[df], Margaret Saunders[c], Lucienne Juillerat-Jeanneret[c], Antonio Marcomini[df], Anna Huk[e], Maria Dusinska[e], Lise M Fjellsbø[e], Francelyne Marano[a] & Sonja Boland[a]

[a] Univ Paris Diderot, (Sorbonne Paris Cité), UMR 8251 CNRS, Unit of Functional and Adaptive Biology (BFA), Laboratory of Molecular and Cellular Responses to Xenobiotics (RMCX), 75205 Paris cedex 13, France,

[b] University Institute of Pathology, UNIL-CHUV, Bugnon 25, CH1011 Lausanne, Switzerland,

[c] Department of Medical Physics & Bioengineering, University Hospitals Bristol NHS Foundation Trust, Bioengineering, Innovation & Research Hub (BIRCH), St Michael's Hospital, Southwell Street, Bristol BS2 8EG, UK,

[d] DAIS-Department of Environmental Sciences, Informatics and statistics, University Ca' Foscari Venice, Dorsoduro 2137, Venice, Italy,

[e] NILU-Norwegian Institute for Air Research, Health Effects Laboratory, Department of Environmental Chemistry, P.O. Box 100, 2027, Kjeller, Norway and

[f] DFBC-Department of Phylosophy and Cultural Heritage, Dorsoduro 3484/D, 30123 Venice, Italy

Published online: 06 May 2015.

http://informahealthcare.com/nan
ISSN: 1743-5390 (print), 1743-5404 (electronic)

Nanotoxicology

Nanotoxicology, 2015; 9(S1): 13–24
 DOI: 10.3109/17435390.2013.829590

informa
healthcare

Toxicity screenings of nanomaterials: challenges due to interference with assay processes and components of classic *in vitro* tests

Rina Guadagnini[1]*, Blanka Halamoda Kenzaoui[2]*, Laura Walker[3]*, Giulio Pojana[4,6], Zuzana Magdolenova[5], Dagmar Bilanicova[4,6], Margaret Saunders[3], Lucienne Juillerat-Jeanneret[3], Antonio Marcomini[4,6], Anna Huk[5], Maria Dusinska[5], Lise M Fjellsbø[5], Francelyne Marano[1], & Sonja Boland[1]

[1]Univ Paris Diderot, (Sorbonne Paris Cité), UMR 8251 CNRS, Unit of Functional and Adaptive Biology (BFA), Laboratory of Molecular and Cellular Responses to Xenobiotics (RMCX), 75205 Paris cedex 13, France, [2]University Institute of Pathology, UNIL-CHUV, Bugnon 25, CH1011 Lausanne, Switzerland, [3]Department of Medical Physics & Bioengineering, University Hospitals Bristol NHS Foundation Trust, Bioengineering, Innovation & Research Hub (BIRCH), St Michael's Hospital, Southwell Street, Bristol BS2 8EG, UK, [4]DAIS-Department of Environmental Sciences, Informatics and statistics, University Ca' Foscari Venice, Dorsoduro 2137, Venice, Italy, [5]NILU-Norwegian Institute for Air Research, Health Effects Laboratory, Department of Environmental Chemistry, P.O. Box 100, 2027, Kjeller, Norway and [6]DFBC-Department of Phylosophy and Cultural Heritage, Dorsoduro 3484/D, 30123 Venice, Italy

Abstract

Given the multiplicity of nanoparticles (NPs), there is a requirement to develop screening strategies to evaluate their toxicity. Within the EU-funded FP7 NanoTEST project, a panel of medically relevant NPs has been used to develop alternative testing strategies of NPs used in medical diagnostics. As conventional toxicity tests cannot necessarily be directly applied to NPs in the same manner as for soluble chemicals and drugs, we determined the extent of interference of NPs with each assay process and components. In this study, we fully characterized the panel of NP suspensions used in this project (poly(lactic-*co*-glycolic acid)–polyethylene oxide [PLGA–PEO], TiO_2, SiO_2, and uncoated and oleic-acid coated Fe_3O_4) and showed that many NP characteristics (composition, size, coatings, and agglomeration) interfere with a range of *in vitro* cytotoxicity assays (WST-1, MTT, lactate dehydrogenase, neutral red, propidium iodide, ^{3}H-thymidine incorporation, and cell counting), pro-inflammatory response evaluation (ELISA for GM-CSF, IL-6, and IL-8), and oxidative stress detection (monoBromoBimane, dichlorofluorescein, and NO assays). Interferences were assay specific as well as NP specific. We propose how to integrate and avoid interference with testing systems as a first step of a screening strategy for biomedical NPs.

Keywords

nanoparticles, nanomedicine, cytotoxicity, oxidative stress, pro-inflammatory response, NanoTEST, testing strategy

History

Received 18 January 2013
Accepted 17 July 2013
Published online 29 April 2015

Introduction

There is an ongoing rapid expansion of nanotechnology, which is becoming increasingly important in society, with the generation of a broad range of consumer products incorporating nanoparticles (NPs) (defined as having at least one dimension <100 nm). These products cover a wide range of areas such as improved chemical processes, environmental remediation, advances in information technology, ''smart'' fabrics, improved drug delivery, medical monitoring, cosmetics, sunscreens, self-cleaning glass, and food packaging (Aitken et al. 2006; Maynard 2007), and are likely to have technological, medical, and economic benefits. Owing to their small size, NPs possess unique properties compared with bulk material, leading to greater surface area per unit mass ratio and hence possibly greater biological reactivity and also quantum effects possibly resulting in novel hazards (Oberdörster et al. 2005a). At present, the human health effects are unclear (EFSA report 2009 of Barlow et al. 2009, SCENIHR report 2009 of Anders et al. 2009), but with the increasing likelihood of population exposure, it is essential that we develop a clear understanding of any risks associated with exposure to nanomaterials. In order to be able to do this, we need a clear understanding of how NPs interact with the biological environment.

In order to relate physicochemical properties to biological interactions and the outcome of a toxicity assay, it is essential that NPs are fully characterized to obtain accurate correlation of results. The characterization of nanomaterials became an issue of concern among researchers as some contradictory toxicological results were reported within the literature. A comprehensive characterization is expected to investigate not only basic parameters such as size distribution and surface area but to also include the study of the NP behavior in biological media (i.e., agglomeration, chemical degradation, etc.) (Oberdörster et al. 2005b; Warheit et al. 2008). A list of physicochemical properties of NPs recommended to be investigated for human health and environmental safety has been proposed by OECD (OECD 2010).

Given the multiplicity of NP types and characteristics, there is a requirement to develop high-throughput screening systems for risk assessment purposes. Cytotoxicity assays provide a common approach for assessing the safety of new chemicals and drugs and

*Equivalent contribution.

Correspondence: Sonja Boland, University Paris Diderot, Sorbonne Paris Cité. Unit of Functional and Adaptive Biology (BFA) CNRS EAC 4413, Laboratory of Molecular and Cellular Responses to Xenobiotics (RMCX), Paris 7, France. Tel: +33 0 1 57 27 84 18. Fax: +33 0 1 57 27 83 29. E-mail: boland@univ-paris-diderot.fr

are generally plate-reader based with readouts that include luminescence, absorbance, fluorescence, time-resolved fluorescence, or fluorescence polarization (Damoiseaux et al. 2011). However, the assessment of the safety of NPs as opposed to soluble chemicals and drugs brings with it a set of specific challenges that must be taken into account as conventional toxicity testing strategies cannot necessarily be directly applied to NPs in the same manner. For rapid high-throughput testing to be feasible, it is essential that the different groups involved in such developments are aware of the unique challenges associated with the application of classical toxicity tests to particles and especially in the area of nanotoxicology.

Unique properties of NPs that can result in interference with conventional toxicity assays include high adsorption capacity, optical properties, hydrophobicity, surface charge, and catalytic activities, requiring the use of appropriate controls and complementary assays (Damoiseaux et al. 2011; Kroll et al. 2009; Griffiths et al. 2011; Doak et al. 2009; Monteiro-Riviere et al. 2009; Stone et al. 2009). Several cytotoxicity assays such as WST-1 metabolization and neutral red (NR) uptake are based on the detection of colored substances by spectrophotometry, and the light refracting or light absorbing capacities of some NPs may interfere with the readout system (Kroll et al. 2012; Stone et al. 2009). This may also affect the quantification of fluorescent probes used to investigate oxidative stress induction. In addition to the optical properties of some NPs, they have been shown to have high adsorption capacities. NPs have been shown to interact with proteins in biological fluids (Lundqvist et al. 2011) and this reactivity of NPs could also lead to interactions with cytokines (Val et al. 2009) or enzymes such as LDH (Han et al. 2011), which may impede their detection for the assessment of the biological effects of NP exposure (Stone et al. 2009). Adsorption of assay reagents or biomolecules depends on NP characteristics such as charge, charge distribution, and hydrophobicity (Turci et al. 2010; Cedervall et al. 2007) as well as curvature (Lundqvist et al. 2004).

Within the EU-funded FP7 NanoTEST project, a range of medically relevant NPs were screened using a broad range of toxicity assays, across cell lines representing up to eight organs, with a view to develop alternative high-throughput testing strategies to assess the toxicological profile of NPs used in medical diagnostics. As part of this process, it has been essential to fully characterize the different NPs and determine the extent of interference with each toxicity assay process and components, and our findings are presented in this study.

Methods

Nanomaterial

Poly(lactic-*co*-glycolic acid)–polyethylene oxide (PLGA–PEO) copolymer water suspension was provided by Advanced *In Vitro* Cell Technologies (Barcelona, Spain). NPs are provided as a 10 mg/ml suspension in water. The investigated nanosized titanium dioxide (TiO_2), an anatase/rutile powder of 21 nm (nominal size), was material-type NM-105 received from the European Commission – Joint Research Centre (Ispra, Italy). This material corresponds to a selected sample of a nanopowder produced by Evonik (Essen, Germany) and marketed as Aeroxide TiO_2 P-25. As TiO_2 NPs were provided as powder, the particles were dispersed in culture media by sonication using an induced ultrasonic probe at 60 W for 3 min (Ultrasonic Processor, Fisher Bioblock Scientific, Illkirch France). Nanomagnetite water dispersions (uncoated (U-Fe_3O_4) or coated with oleic acid (OC–Fe_3O_4)) were purchased from Plasmachem (Berlin, Germany). NPs were provided as a 28 mg/ml (U-Fe_3O_4) or 260 mg/ml (OC–Fe_3O_4) suspension in water and diluted in phosphate buffer saline (PBS) to obtain a final concentration of 2 mg/ml. Amorphous silica was purchased from Corpuscular INC (Cold Spring, USA) as a water dispersion of rhodamine labeled 25 nm (Fl-25 SiO_2) or 50 nm (Fl-50 SiO_2) diameter silica. All NPs were diluted after vortexing in culture medium at concentrations corresponding to 75 μg/cm^2. The equivalence in milligram per milliliter depends on the assay used and is indicated in each description of the method. Serial 1/5 dilutions were performed for some assays down to 0.6 μg/cm^2.

Characterization of nanoparticles

Investigated NPs were characterized in detail by a combination of analytical techniques. The mean average size of primary particles was determined by TEM (transmission electron microscope) analysis with a Jeol 3010 TEM operating at 300 kV. Surface area and pore volume were obtained by nitrogen adsorption on a Micromeritics ASAP2000 Accelerated Surface Area and Porosimetry System at an adsorption temperature of −196 °C, after pretreating the sample under high vacuum at 300 °C for 2 h (Brunauer et al. 1938). Actual concentrations of Fe_3O_4 NPs in batches provided were determined by atomic absorbance spectroscopy (AAS) after acid digestion of sample aliquots. Dynamic light scattering (DLS) analysis and zeta potential of provided dispersions, as well as of NP dispersions in culture media were determined with a submicron particle sizer Nicomp 380 equipped with a 35 m W He–Ne laser 632.8 nm laser diode and photodiode detector set at 90° (PSS, FL, USA). Suspensions of NPs investigated in biological media were freshly prepared according to different protocols specifically developed for each NP type. Stock dispersion was added to cell culture media to achieve a 75 μg/cm^2 working solution and concurrently analyzed by DLS. Other characterization data about other properties of the selected NPs are reported in the paper on characterization of NPs in this special issue (Dusinska et al. 2015).

Cell lines and cell cultures

The immortalized human alveolar epithelial cell line A549 was provided by ATCC (LGC Standards, Molsheim, France) and grown in DMEM-F12 (Dulbecco Modified Eagle medium Nutrient Mix F-12) cell culture media supplemented with 1% Glutamax and 10% fetal calf serum (FCS) (all reagents purchased from Invitrogen, Cergy Pontoise, France).

The kidney fibroblast cell line Cos-1 was maintained in DMEM medium (1000 mg/L glucose) (Sigma) containing 10% fetal bovine serum (FBS), 100 U/ml penicillin, and 100 mg/ml streptomycin.

EC219 rat brain endothelial cells previously developed and characterized (Juillerat-Jeanneret et al. 1992) were grown in DMEM medium containing 1.0 g/L glucose, 10% FCS, and penicillin/streptomycin antibiotics (all reagents purchased from Gibco, Invitrogen, Basel, Switzerland).

All cells were cultivated in 25 cm^2 and 75 cm^2 flasks in an incubator at 37°C and 5% CO_2 in a humidified atmosphere, and culture media was changed every 2–5 days. Adherent cells were routinely subcultured every 2–7 days by detaching cells with trypsin (0.05%)–EDTA (ethylene diamine tetracetic acid) (2 mg/ml Invitrogen). Enzymatic activity of trypsin was inhibited by the addition of 10% FCS. Cells grown in a suspension were routinely diluted to 2×10^5–1×10^6 cells/ml.

Neutral red assay

Subconfluent cell cultures of A549 in 96-well culture plate (Costar) were rinsed with PBS (Invitrogen). NR (Sigma–Aldrich, Saint-Quentin Fallavier, France) at 0.0025% in DMEM/F12

(without phenol red, containing Hepes; Invitrogen) was added and the plate was incubated for 3 h at 37°C and 5% CO_2. After rinsing the cells twice with PBS, the plates were lysed by incubation with 1% acetic acid (VWR, Fontenay-sous-Bois, France) and 50% pure ethanol (VWR) in water for 40 min at room temperature (RT) under agitation and protected from light. The extracts were transferred to a plate without cells but containing NPs at 75 μg/cm^2 (240 μg/ml), which were pre-incubated in culture media for 24 h at 37°C and 5% CO_2. Optical density (OD) was determined at 550 nm using a multiwell plate reader (FluoStar Galaxy plate reader BMG Labtechnologies, Champigny sur Marne, France). A blank without cells containing a solution of 1% acetic acid and 50% pure ethanol in water was used for background correction.

MTT Assay: The EC219 cells were seeded in a Petri dish (Nunclon, Milian, Geneva, Switzerland) in their standard culture medium and grown until confluent. MTT (3-(4,5-dimethylthiazol-2-yl)-2,5-diphenyl-tetrazolium bromide, Sigma–Aldrich Buchs, Switzerland) dissolved in PBS (5 mg/ml) was added at a 1:25 ratio, and after 2 h of incubation at 37°C, cells were lysed and precipitated formazan dissolved in 0.4N HCl in isopropanol. The NPs were prepared in 0.4N HCl in isopropanol or in formazan obtained from EC219 cells lysed in 0.4N HCl in isopropanol at 250 μg/ml (concentration corresponding to 75 μg/cm^2). The absorbance of these solutions was measured immediately at 540 nm and compared to blanks (no NP addition) using a multiwell plate reader (iEMS Labsystems, BioConcepts, Allschwil, Switzerland).

WST-1 assay

A549 cells were cultured to subconfluence in 96-well culture plate (Costar). Cells were incubated in DMEM/F12 (without phenol red, containing Hepes) with WST-1 reagent (Roche Diagnostics, Meylan, France) for 2 h, and supernatants were transferred to a plate without cells but containing NPs that were pre-incubated at 75 μg/cm^2 (240 μg/ml) in culture media for 24 h at 37°C and 5% CO_2. OD was determined immediately in a multiwell plate reader at 450 nm (Bio-Tek EL 808, Bio-Tek Instruments Inc, Colmar, France). For cytotoxicity studies, cells were exposed to NPs at 75 μg/cm^2 for 24 h, washed with culture media, and incubated with WST-1 for 2 h. OD was measured at 450 nm against a blank without cells but containing culture media and WST-1. Supernatants were then transferred to a new plate and analyzed again in the plate reader.

LDH assay

Interference of NP solutions with the lactate dehydrogenase (LDH) assay (Promega, UK) was assessed using LDH enzyme positive control (supplied in kit) at 1:5000 final dilution. NP solutions were dispersed and diluted into the desired working concentrations of 75 μg/cm^2 (480 μg/ml) in DMEM-F12-HAM medium (Sigma–Aldrich, UK) in the presence or absence of LDH and incubated in 96-well plates (Corning, UK) at 37°C in a humidified 5% CO_2 atmosphere for 24 h. After incubation, 50 μl supernatant was removed from each well and transferred to a fresh transparent 96-well plate. Plates were incubated with LDH assay buffer for 30 min at 37°C and 5% CO_2 and then read on a FluoSTAR OPTIMA fluorescence microplate reader from BMG Labtech (Aylesbury, UK) at 492 nm, as per manufacturer's instructions.

PI uptake

Cells were seeded at 15×10^3 cells/cm^2 in 12-well plates, grown for 48 h, and then exposed for 24 h at 37ºC to NPs at 75 μg/cm^2 (407 μg/ml) in culture media without phenol red. Supernatants were sampled in cytometry tubes and cells are detached by the addition of 500 μL trypsin–EDTA (Invitrogen) and blocked with +10% FCS (Invitrogen). Cells were added to supernatants, and propidium iodide (PI, Sigma–Aldrich, 5 μg/ml final concentration in culture medium) was added a few minutes before cytometric analysis. A total of 7000 viable or dead cells were analyzed using a CyAn ADP LX flow cytometer (Dako Cytomation, Beckman Coulter, Villepinte, France). Laser excitation and emission bandpass wavelengths were 488 nm and 620 ± 30 nm, respectively.

Cell counting

A total of 10 μl of NP suspensions at 270 μg/ml (corresponding to a concentration of 56.25 μg/cm^2) was mixed with 10 μl of trypan blue (0.4%, Invitrogen) and counted automatically using a cell counter (Countess® Automated Cell Counter, Invitrogen).

Thymidine incorporation assay

^{3}H-Thymidine (^{3}H-T) incorporation assay was performed in untreated EC219 cells, as previously described (Halamoda Kenzaoui et al. 2012). Radioactivity was counted in a β-counter (WinSpectra, Wallac, Germany). The NPs were then added to the radioactivity tubes at 160 μg/ml (concentrations corresponding to 75 μg/cm^2), and the counting measurement was repeated. The radioactivity counts in the presence of NPs were compared to the radioactivity counts before the addition of the NPs.

Immunotoxicity assays: adsorption of IL-6, IL-8, and GM-CSF cytokines on NPs

The 48-well culture plates (Costar, France) were coated with a solution of 0.3% BSA (bovine serum albumin, Sigma–Aldrich, France) in DMEM/F12 (without phenol red, containing Hepes) and incubated for 15 min at 37°C and 5% CO_2. After rinsing for three times with the culture media, 150 μl of cytokines at 500 pg/ml (IL-6, IL-8, and GM-CSF standards from DuoSet ®ELISA Kit, R&D Systems, Lille, France) were added in culture media. A total of 150 μl of NP dispersions was added to obtain a concentration of 75 μg/cm^2 (237.5 μg/ml) before incubation for 24 h at 37°C and 5% CO_2. Supernatants were centrifuged at 10,000 rpm for 10 min at 4°C and supernatants stored at −80°C. Concentration of cytokines in the supernatants was evaluated using the DuoSet® ELISA Kit (R&D Systems). The OD was determined at 450 nm by a multiwell plate reader (Dynex, MRX; Thermolab systeme, Cergy Pontoise, France).

Monobromobimane assay

The NP suspensions at 250 μg/ml (corresponding to 75μg/cm^2) were prepared in TritonX-100 0.01% in HBSS (Hank's buffer solution containing 1.3 mM Ca^{2+}, 1.1 mM Mg^{2+}, and 5 mM glucose, Gibco, Invitrogen, Basel, Switzerland) in 48-well plates (Costar Corning, NY, USA). Monobromobimane (mBBr) was added to wells at a final concentration of 10 μM, and fluorescence was measured immediately at 360/460 nm in a fluorescence plate reader (CytoFluor Series 4000, PerSeptive Biosystems, MA, USA).

H_2DCF-DA oxidation assay

The NP suspensions at 250 μg/ml (corresponding to 75μg/cm^2) were prepared in enriched HBSS and added as triplicates in the wells of a 48-well plate (Costar, Switzerland). 5/6carboxy-2,7-dichloro-dihydro-fluorescein diacetate (Carboxy-H_2DCF-DA, Molecular Probes, Invitrogen Basel, Switzerland, stock solution 25 mg/ml in DMSO) was added to each well at a final

concentration of 20 μM, and the plate was read at $\lambda_{ex}/\lambda_{em} = 485/530$ nm in a fluorescence plate reader (CytoFluor Series 4000) at $t = 0$ h, then every hour for 4 h.

NO determination

The NP suspensions at 250 μg/ml (corresponding to 75 μg/cm^2) were prepared in complete culture medium of EC219 and added to wells of a 48-well plate (Costar, Switzerland). After 24-h incubation at 37°C, 100 μl of the supernatants was transferred into the wells of a 96-well plate (Costar, Switzerland), and 100 μl of the Griess reagent (0.5 mg/ml naphthylethylenediamine and 5 mg/ml sulphanilamide in 5% H_3PO_4) prepared immediately before use was added. After 5–10 min of incubation at RT the absorbance was measured at 540 nm using a multiwell plate reader (iEMS Labsystems, BioConcepts, Allschwil, Switzerland) and compared with the blank (culture media without NP addition).

Statistical analysis

Data are represented as mean ± SD and were analyzed using Sigma Stat software by analysis of variance (ANOVA) followed by Dunnett's test or Student–Newman–Keuls.

Results

Particle characterization

A detailed physical and chemical characterization of the selected NPs has been performed. A wide combination of analytical techniques was employed, including TEM, BET, and DLS. Table I summarizes the main characterization data obtained for the investigated NPs. Since the BET technique could be applied only to powdered samples, a preliminary evaporation step was investigated in order to extend this technique to Fe_3O_4 suspensions without affecting the particle surface structure. The best procedure proved to be a very slow evaporation at RT before pretreatment under N_2 flow. This procedure could not be applied to OC–Fe_3O_4 and PLGA–PEO suspension as additives or stabilizers could coat the particles during the evaporation process. In addition to primary characterization, additional investigations were performed in order to ascertain possible impurities of toxicological concern in the selected NPs. The coating of OC–Fe_3O_4 was found to be made of technical quality sodium oleate (data not shown). No further contaminants of toxicological concern were detected in the selected NPs.

Characteristics of NP dispersions in culture media

Typical secondary (i.e. behavior in culture media) properties, such as size distribution and size stability toward agglomeration of selected NPs are reported in Table II. The reported data refer to behavior in DMEM–F12–HAM as a representative example of culture media. Only the SiO_2 NPs show size distributions (determined by DLS) very similar to their actual particle size as determined by TEM. All other NPs exhibited instead a bimodal distribution, with a peak in the nanorange (similar to TEM-size) and another agglomerate peak at larger, non-nano (i.e. >100 nm) size range (TiO_2, PLGA, and OC–Fe_3O_4), or formation of very large agglomerates with sizes even in the micrometer range (U-Fe_3O_4). U-Fe_3O_4 proved to be very unstable with respect to agglomeration, exhibiting size distributions that rapidly increase in less than 5 min. All other NPs were shown to be stable for at least 1 day, indicating the feasibility of *in vitro* testing without influence from potential agglomeration. However, the dispersion protocol had a strong influence on the size of agglomerates and time stability of dispersions, as recently reported within the literature for TiO_2 NPs (Magdolenova et al. 2012).

Table II. Typical secondary characteristic properties and size stability toward agglomeration in DMEM-F12-HAM culture medium of selected NPs.

	TiO_2	PLGA–PEO	OC–Fe_3O_4	U-Fe_3O_4	Fl-25 SiO_2	Fl-50 SiO_2
pH in original suspension	- [1]	2.75	5.95	2.64	7.98	7.76
Zeta potential in milliQ water at pH 7 (mV)	−30.2	−43.4	−31.9	−2.8	− 20	− 22
Average size in original suspension−DLS	− [1]	110 and 390 nm	− [2]	− [2]	26 nm	38 nm
Average hydrodynamic diameter in culture media−DLS	Large agglomerates: Bimodal distribution: 101 nm, 278 nm	Bimodal distribution: 112 nm, 351 nm	Bimodal distribution: 31 nm, 132 nm	Large agglomerates: 1–50μm	26 nm	40 nm
Size stability (by DLS)	2 days	∼1 day	∼3 days	<5 min	<1 day	<1 day

[1]Not applicable; [2]Too high concentration for DLS measurement.

Table I. Summary of primary physical and chemical properties of selected nanoparticles.

	TiO_2	PLGA-PEO	OC–Fe_3O_4	U-Fe_3O_4	Fl-SiO_2 25	Fl-SiO_2 50
Phase	Powder	Water dispersion	Water dispersion	Water dispersion	Water dispersion	Water dispersion
Crystal structure	Anatase/rutile	- [1]	Spinel (octahedral)	Spinel (octahedral)	Amorphous	Amorphous
Chemical composition-TEM/EDX	Ti, O	C, H, O	Fe, O	Fe, O	Si, O	Si, O
Primary size (nm)	15–60 [2]	100–1200 [2]/ 143 [3]	9 × 7 [4]	10 × 7 [4]	15–30 [2]	25–50 [2]
Purity of particles (%)	>99	- [1]	>99	>99	>99	>99
Particle concentration (%)[1]	- [1]	0.33	26	2.8	1.4	1.2
Shape-TEM	Irregular	- [1]	Oblong	Oblong	Round/oblong	Round/oblong
Crystallite size distribution-TEM (nm)	15–60	- [1]	5–12	5–13	15–30	25–50
Surface area-BET (m^2/g)	61	- [1]	- [1]	92	159	87
Pore volume-BET (ml/g)	0.13	- [1]	- [1]	- [1]	- [1]	- [1]
Surface chemistry	Uncoated	Uncoated	Oleate micelle coating	Uncoated	Uncoated	Uncoated

[1]Not applicable; [2]By TEM; [3]By DLS; [4]Oblong shape.

Interference of NPs with toxicity assays

We tested the interference of NP dispersions with different toxicological assays in acellular conditions or using untreated cells. We generally performed pre-incubation of NPs with media to mimic the conditions of toxicity assays. Different time-points and concentrations were used but we show here only the results after 24 h of treatment at 75 μg/cm^2, the highest concentration used in the NanoTEST project for *in vitro* toxicity screening.

Cytotoxicity assays

The following assays were used to evaluate cytotoxicity: NR, MTT, WST-1, LDH, Thymidine incorporation, PI uptake, and cell counting.

We evaluated the interference between NPs and NR which is taken up into lysosomes of viable cells. Untreated cells were exposed to NR, then extracted, and the NR-cell extracts were incubated with the selected NPs. The changes in OD readings were compared to determine the effects of NPs on OD measurements (Figure 1). It was obvious that neither PLGA–PEO nor SiO_2 NPs interfered with the detection of NR dye. TiO_2 and Fe_3O_4 NPs induced a great increase in OD, and coating Fe_3O_4 NPs with oleic acid further increased the OD. Decreases in OD readings were also observed at 3 μg/cm^2 but not at 0.6 μg/cm^2 for these three NPs (TiO_2, U-Fe_3O_4 and OC–Fe_3O_4). To evaluate the cytotoxicity of NPs on cells, the NR dye has to be extracted from cells, which results in the liberation of NPs which will be present during the spectrophotometric analysis. In the case of Fe_3O_4 or TiO_2 NPs, this could thus lead to false negative results.

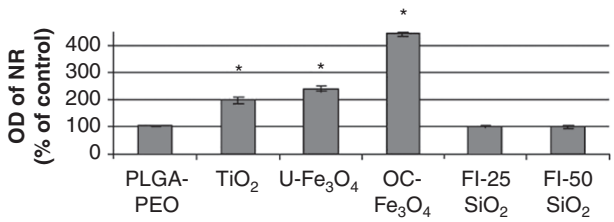

Figure 1. Interference of NPs with the Neutral Red assay. Optical density at 550 nm of NR dye extracted from untreated A549 cells after addition of NPs at 75μg/cm^2 just before spectrophotometric analysis. Results ($n = 6$) are expressed as % of control (OD of NR in the absence of NPs). *Significantly different from the control ($p < 0.05$ ANOVA followed by Dunnett's test).

Other cytotoxicity assays are based on the measurement of the metabolic activity of the cultures by evaluating the transformation of tetrazolium salts into formazan. However, it has been shown that some NPs could interfere with formazan salts (Wörle-Knirsch et al. 2006). Therefore, it is important to verify if there is any interaction between the selected NPs and formazan detection before performing viability tests on cells treated with NPs. We thus added the tetrazolium salt MTT to unexposed cells, which reduce it to formazan, extracted it in iPrOH/HCl and quantified it by spectrophotometry. The absorbance of the NP dispersions was measured in iPrOH/HCl with or without the dissolved formazan to evaluate the influence of the NPs on OD readings in both solutions (Figure 2A and B). The presence of TiO_2 NPs and both Fe_3O_4 NPs increased the absorbance of the solutions. However, the increase of absorbance was more significant for the NPs in iPrOH/HCl solutions than in formazan solutions. An increase of OD readings could also be observed from 3 μg/cm^2 in iPrOH/HCl and from 15 μg/cm^2 in the presence of formazan. Neither SiO_2 NPs influenced the OD readings in our tests. The PLGA–PEO

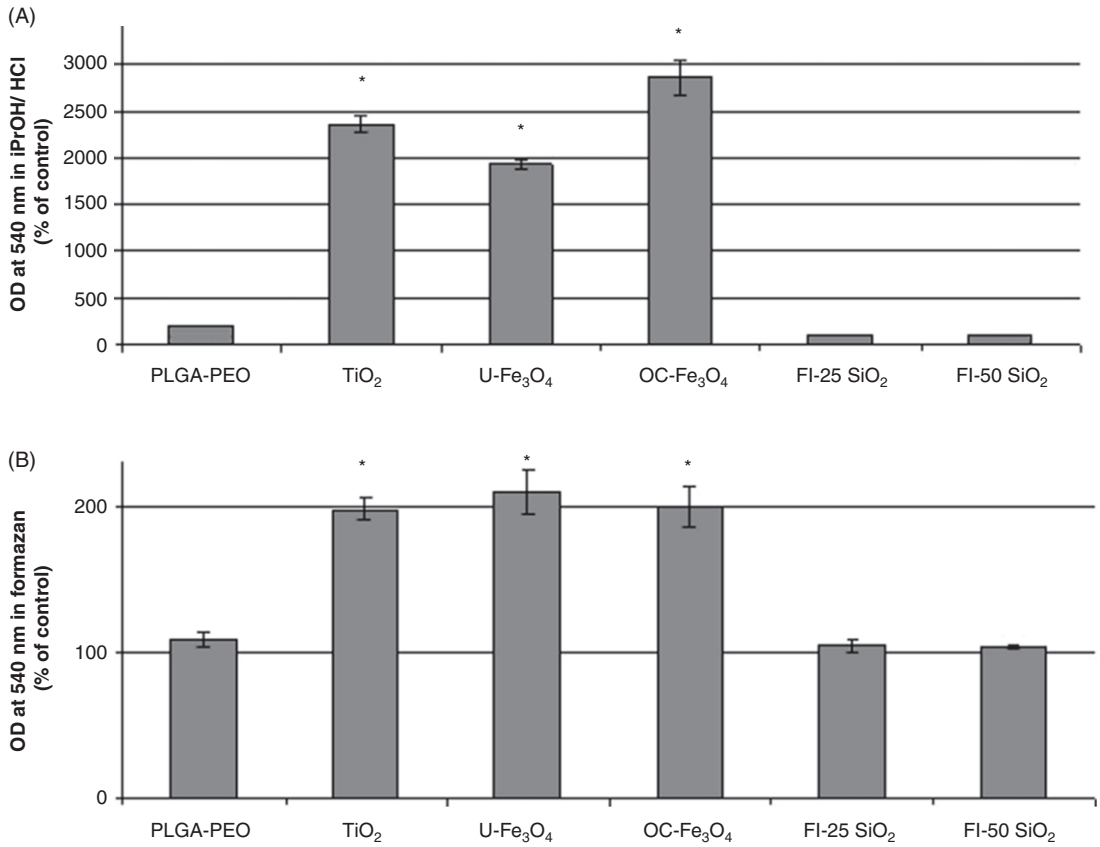

Figure 2. Interference of NPs with the MTT assay. Optical density at 540 nm of A) iPrOH/HCl or B) MTT extracted in iPrOH/HCl from untreated EC219 cells after addition of NPs at 75μg/cm^2 just before spectrophotometric analysis. Results ($n = 3$) are expressed as % of control (OD at 540nm in the absence of NPs). *Significantly different from the control ($p < 0.05$ ANOVA followed by Dunnett's test).

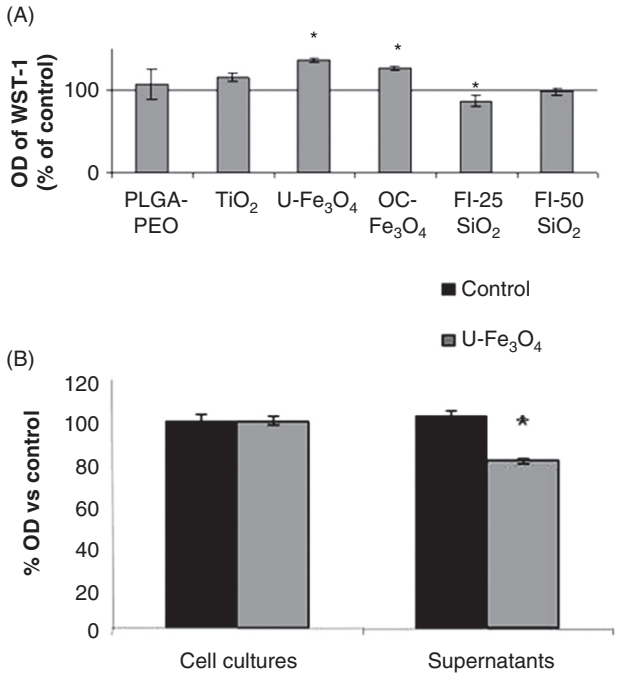

Figure 3. Interference of NPs with the WST-1 assay. A) Detection of WST-1 in the presence of NPs. Optical density at 450 nm of WST-1 from untreated A549 cells after addition of NPs at 75μg/cm^2 just before spectrophotometric analysis. Results ($n = 6$) are expressed as % of control (OD of WST-1 in the absence of NPs). *Significantly different from control ($p < 0.05$ ANOVA followed by Dunnett's test). B) Cytotoxicity of U-Fe_3O_4 NPs evaluated by quantifying formazan formation on cell cultures or supernatants. Optical density at 450 nm of WST-1 from A549 cells treated with U-Fe_3O_4 NPs at 75 μg/cm^2 for 24 h evaluated directly on cell cultures or on their supernatants alone. Results ($n = 6$) are expressed as % of control (OD of WST-1 of untreated cells). *Significantly different from control ($p < 0.05$ ANOVA followed by Dunnett's test).

NPs did not have a significant effect on absorbance measurements in formazan solution, whereas in iPrOH/HCl their maximal concentration slightly increased the OD readings but this was not observed at 15 μg/cm^2. The results obtained suggest that the presence of metallic NPs in samples can blunt their potential cytotoxic effect due to particle interference with OD readings. The water soluble tetrazolium salt WST-1, in contrast to MTT, is released into the supernatants and detected at 450 nm instead of 540 nm. We thus measured the OD of supernatants of untreated cells incubated with WST-1, after addition of NPs just before spectrophotometric readings. Our results (Figure 3A) show that Fe_3O_4 NPs interfere with WST-1 measurements by significantly increasing the OD. This interference was also observed from 15 μg/cm^2 for OC–Fe_3O_4 whereas U-Fe_3O_4 only increased the OD at 75 μg/cm^2. WST-1 is a water-soluble tetrazolium salt which is released into the supernatant, and the presence of Fe_3O_4 NPs during the spectrophotometric analysis may thus be avoided by measuring the OD of the supernatants once moved into fresh wells if the NPs have been eliminated before adding the WST-1 reagent. To verify whether this adaptation of the protocol prevents interference during cytotoxicity tests on cells treated for 24 h with these NPs, we transferred supernatants after incubation with WST-1 reagent in a new plate and compared the OD of these supernatants with the measurements performed on cell cultures just before the transfer. Figure 3B shows that without transferring the supernatants to a new plate, the OD of cells treated with 75 μg/cm^2 of U-Fe_3O_4 NPs is the same as control cultures and these NPs do not seem to be toxic. However, the OD of the supernatants alone, containing virtually no particles due to extensive rinsing, indicates a decrease of the metabolic activity compared to untreated cultures. Thus, the presence of NPs during the spectrophotometric measurements could lead to an underestimation of their toxicity, but analysis of NP-free supernatants may prevent false negative results if they contain no NPs.

Membrane damage due to toxicity can be investigated by measuring the release of the cytoplasmic enzyme LDH into the cell culture supernatants. However, NPs may interfere with the LDH detection assay either during OD measurements or by adsorption of the enzyme on NP surfaces. Interference of NPs with the LDH assay is easily assessed due to the provision of LDH enzyme as a positive control in the kit. Figure 4 shows only very slight interferences with NPs, indicating that this test could be used to assess NP cytotoxicity.

Cytotoxicity can also be assessed by quantifying cell proliferation. Thymidine incorporation could be used to study DNA synthesis by cells. The radioactivity of incorporated ^{3}H-thymidine is counted in cell extracts, though the presence of NPs in samples can potentially modify the count values. Therefore, after counting the radioactive extracts of unexposed cells, NPs were added to the tubes and the measurements were repeated in order to compare the values before and after NP addition. Among the NPs tested both Fe_3O_4 NPs decreased the beta-counts at 56.25 μg/cm^2 (Figure 5). A decrease could also be observed at 25 μg/cm^2 for OC–Fe_3O_4 and 60 μg/cm^2 for U-Fe_3O_4. TiO_2 and SiO_2 NPs did not modify the radioactivity counts. Another way to quantify cell proliferation is to count exponentially growing cells at distinct time intervals, most commonly every 24 h and to compare proliferation of exposed with unexposed cells. Cell counting by automated cell counters (Countess®) is critical, compared to manual counting of cells as every particle (or agglomerate) with similar size as the cells will be recognized by the counter. Figure 6A indeed shows that iron oxide NPs are recognized as cells (7.5 10^4 false cell counts/ml at 56.25μg/cm^2) but the number counted as false cells is very small. As generally 5–10 $\times$ 10^5 cells are counted by this device, the NP agglomerates will represent less than 10% when counting treated cells. Interestingly, U-Fe_3O_4 NPs are counted as living cells (Figure 6B) which will increase the number of total cells and falsely appear to increase viability leading to an underestimation of cytotoxicity. In contrast, OC–Fe_3O_4 NPs are recognized as dead cells which could thus give an overestimation of cell death. Automatic cell counters such as Countess® can thus give false results, as NPs in suspension could agglomerate, especially at high concentration or in serum-rich media. Before the start of experiments, it is recommended to check if NPs are detected by the automatic cell counter (this should be checked at a higher NP concentration than that used for experiments). Counting of NPs as cells is also critical in flow cytometric analysis, where they can however be excluded by gating. Figure 7 shows the cytotoxicity evaluation by PI incorporation after alteration of membrane integrity. The percentage of dead cells determined by quantifying cells fluorescently labeled with PI could be underestimated if NP agglomerates are not excluded from the analysis, to avoid counting them as viable cells. The analysis of PI intensity (PI log) versus the size of the fluorescent event (FS area) allows a gate of cell debris and NPs to be established, which could thus be excluded from the analysis.

Pro-inflammatory response

The pro-inflammatory response induced in cells can be evaluated by measuring the secretion of cytokines in the supernatants. However, it is well known that proteins can be adsorbed on NP surfaces (Val et al. 2009; Xu et al. 2010; Turci et al. 2010), and it is necessary to verify whether the cytokines secreted after

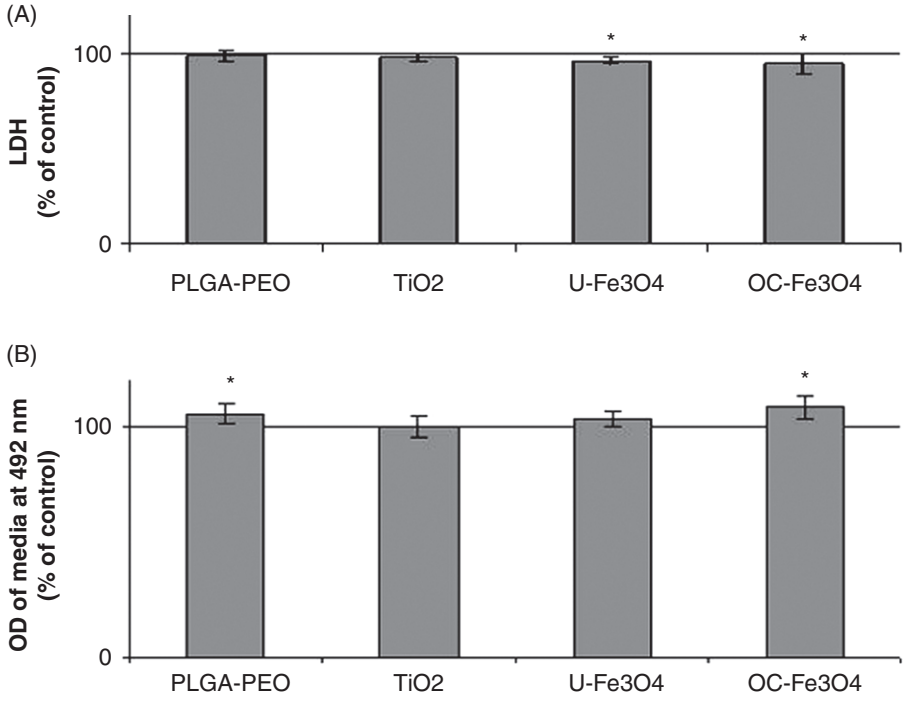

Figure 4. Interference of NPs with the LDH assay. Optical density at 492 nm of A) LDH incubated in culture media for 24h with NPs at 75 μg/cm^2 B) Culture media without enzyme incubated for 24h with NPs at 75 μg/cm^2 before spectrophotometric analysis. Results ($n = 6$) are expressed as % of control (LDH incubated in the absence of NPs or buffer without NPs).

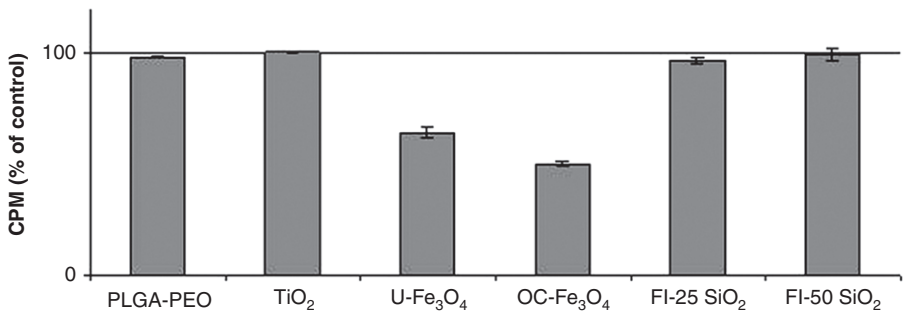

Figure 5. Interference of NPs with the thymidine incorporation assay. Radioactivity counts (CPM) of [^{3}H]-Thymidine from untreated EC219 cells after addition of NPs at 75μg/cm^2 just before β-counting. Results are expressed as % of control (CPM in the absence of NPs).

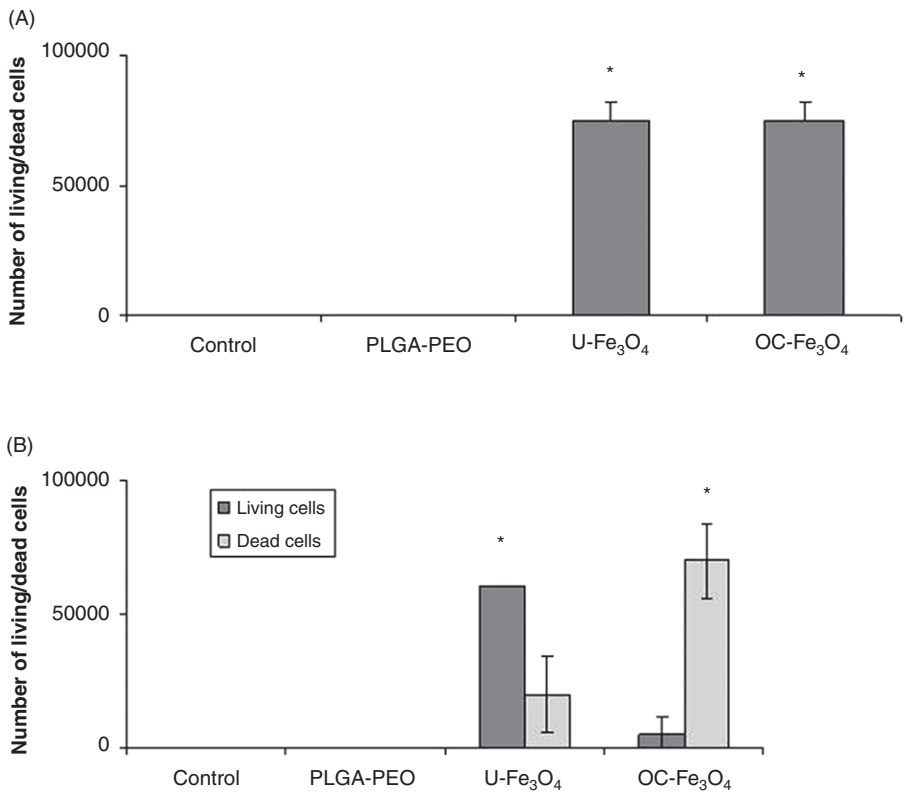

Figure 6. Interference of NPs with automatic cell counting. Number of cells identified by Countess® automatic cell counter in NP dispersions incubated for 24h at 56.25μg/cm^2 in the absence of cells ($n = 2$). A) Total countsper milliter B) Living and dead cell counts/mL. *Significantly different from control ($p < 0.05$ ANOVA followed by Student-Newman-Keuls test).

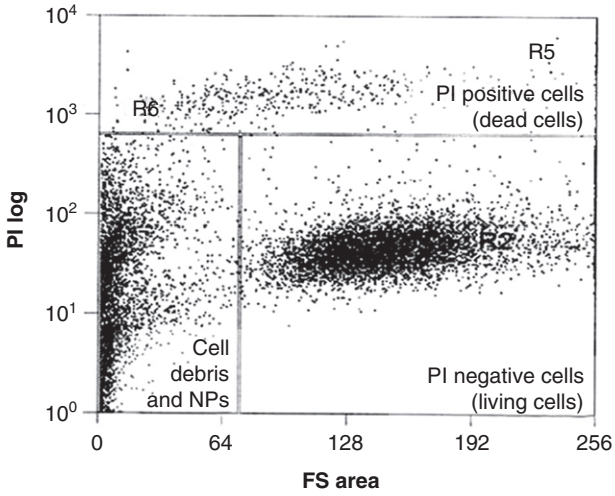

Figure 7. Interference of NPs with the Propidium Iodide assay. Plot of cytometric analysis of A549 cells exposed for 24h to TiO_2 NPs. Fluorescence intensity of PI at 488/620 nm excitation/emission wavelength (PI Log) versus size of the anaysed fluorescent event (Forward Scatter (FS) area).

exposition to NPs can be adsorbed onto these NPs. IL-6, IL-8, or GM-CSF were incubated with NPs at 75 μg/cm^2 for 24 h in acellular conditions and after elimination of particles by centrifugation we quantified the remaining cytokines by ELISA. The results in Figure 8 show that all NPs adsorb cytokines except PLGA–PEO NPs, which increases the apparent concentration of cytokines. For the other NPs, the level of adsorption depends on the NP and the cytokine studied. OC–Fe_3O_4 NPs are the most cytokine-adsorbing NPs tested as cytokines could not be detected in the supernatants. U-Fe_3O_4 NPs highly adsorbs IL-6 and IL-8 whereas GM-CSF was less but however still significantly adsorbed. TiO_2 NPs also adsorbs all tested cytokines but less than U-Fe_3O_4 NPs. The adsorption on SiO_2 depends on the size of the NP as the smaller Fl-25 SiO_2 NPs were more cytokine-adsorbing than the larger Fl-50 SiO_2 NPs. Adsorption of cytokines could also be observed at 15 μg/cm^2 but lower concentrations were not assessed.

Detection of oxidative stress

Generation of oxidative stress in cells can be evaluated by the measurement of the intracellular production of reactive oxygen species (ROS) (by detecting H_2DCF-DA oxidation) or by the quantification of the cellular thiol levels (using the monobromobimane (mBBr) assay). These tests are based on fluorescence measurements, which can be modified by the presence of NPs in wells and consequently give false-negative or false-positive results. The production of the free radical nitric oxide could also result in an oxidative stress. NO production could be quantified indirectly by a colorimetric method using the Griess reagent.

The mBBr assay measures thiol levels in cells by forming highly fluorescent thioether units with fluorescence excitation/emission 360/460 nm. According to our results (Figure 9), while Fe_3O_4 NPs present in samples during the fluorescence measurement can significantly decrease the fluorescence signal, TiO_2 NPs increase the fluorescence values at 75 μg/cm^2. The effects of Fe_3O_4 were also observed at lower concentrations (0.6 μg/cm^2 for OC–Fe_3O_4 and 15 μg/cm^2 for U-Fe_3O_4) but no interference of TiO_2 NPs was noticed at these lower concentrations. PLGA–PEO and SiO_2 NPs did not influence the fluorescence measurements in our tests.

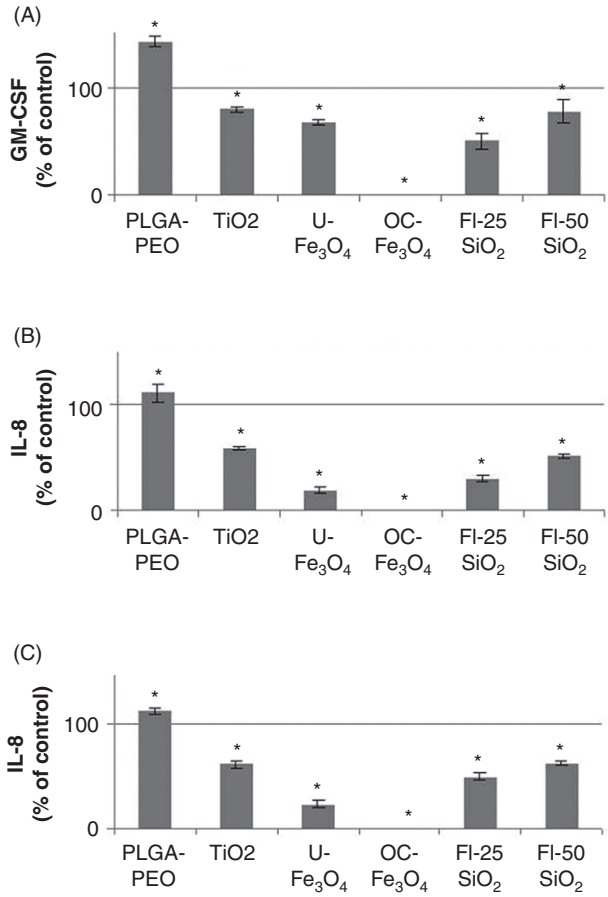

Figure 8. Interference of NPs with ELISA A) GM-CSF. B) IL-6 and c) IL-8 were quantified by ELISA after 24h of incubation with NPs at 75 μg/cm^2 after elimination of particles by centrifugation. Results ($n = 6$) are expressed as % of control (cytokine incubated in the absence of NPs). *Significantly different from the control ($p < 0.05$ ANOVA followed by Dunnett's test).

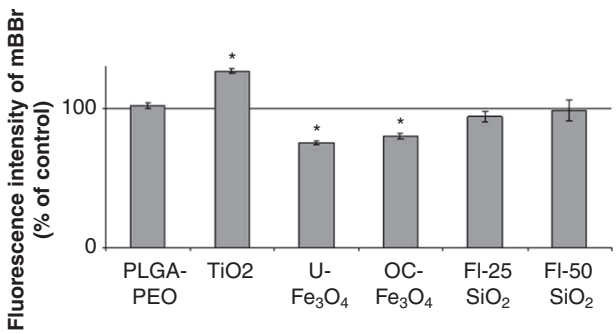

Figure 9. Interference of NPs with the monobromobimane assay. Fluorescence intensity of mBBr at 360/460 nm excitation/emission wavelength after addition of NPs at 75μg/cm^2 just before fluorimetric analysis. Results ($n = 3$) are expressed as % of control (Fluorescence at 460nm in the absence of NPs). *Significantly different from the control ($p < 0.05$ ANOVA followed by Dunnett's test).

The intracellular production of ROS can be evaluated using H_2DCF-DA which, after intracellular deacetylation by esterases, can be oxidized by ROS and transformed into fluorescent dichlorofluorescein (DCF) with fluorescence excitation/emission at 485/530 nm. The presence of TiO_2 NPs in the samples during measurement increases the fluorescence intensity (Figure 10) whereas U-Fe_3O_4 and OC–Fe_3O_4NPs decrease the

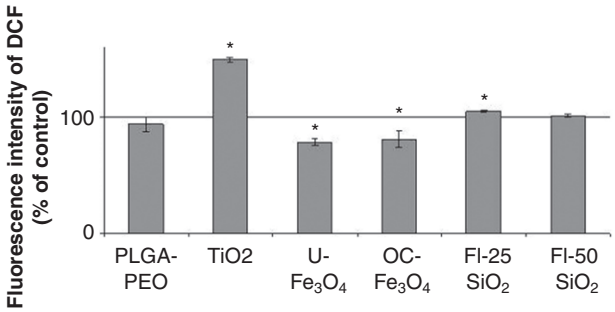

Figure 10. Interference of NPs with the H_2DCF-DA oxidation assay. Fluorescence intensity of DCF at 485/530 nm excitation/emission wavelength after addition of NPs at 75μg/cm^2 just before fluorimetric analysis. Results ($n = 3$) are expressed as % of control (Fluorescence at 530nm in the absence of NPs). *Significantly different from the control ($p < 0.05$ ANOVA followed by Dunnett's test).

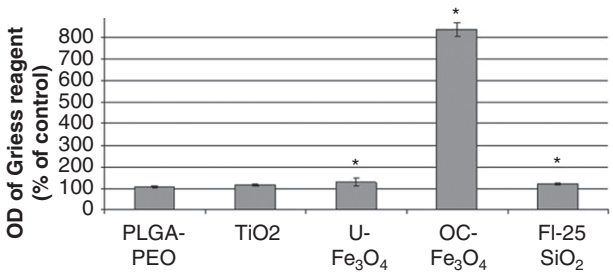

Figure 11. Interference of NPs with the NO detection assay. Optical density at 540 nm of Griess reagent after 24 h of incubation with NPs at 75 μg/cm^2. Results ($n = 3$) are expressed as percentage of control (OD of Griess reagent in the absence of NPs). *Significantly different from the control ($p < 0.05$ ANOVA followed by Dunnett's test).

fluorescence values. This decrease in fluorescence could be observed at 0.6 μg/cm^2 for OC–Fe_3O_4 and at 15 μg/cm^2 for U-Fe_3O_4, whereas the increase in presence of TiO_2 was not detected at these concentrations.

Exposure to toxicants could also lead to the production of the free radical nitric oxide. NO production by cells could be measured in cell culture supernatants as the stable metabolite nitrite (NO_2^-) reacts with the Griess reagent generating a purple-azo dye product that can be monitored by a spectrophotometer at 540 nm. The presence of NPs in cell culture supernatants can modify the OD readings depending on the NP type (Figure 11). OC–Fe_3O_4 NPs enhance the absorbance readings to a very great extent whereas U-Fe_3O_4 only slightly increased the OD and interference could also be observed at 0.6 μg/cm^2 for OC-Fe_3O_4 but only at 75 μg/cm^2 for U-Fe_3O_4. These differences may be due to the fact that they are much less stable in cellular environment and agglomerates quickly sediment on the bottom of the wells. SiO_2 NPs also slightly increased OD values, whereas TiO_2 and PLGA–PEO NPs did not show any interference with this test.

Discussion

In this study we evaluated the interference of a panel of NPs (PLGA-PEO, TiO_2, two sizes of SiO_2, uncoated and oleic acid coated Fe_3O_4 NPs) with several *in vitro* cell assays in order to determine which assays are suitable for the testing of NPs in cell models, and to adapt the protocols if necessary, as a basis to develop a testing strategy for NPs used in medical applications. Several studies have already shown interference of NPs with *in vitro* assays but mostly using carbon-based materials (Kroll et al. 2012; Monteiro-Riviere et al. 2009; Wörle-Knirsch et al. 2006), whereas studies on NPs for biomedical applications are still warranted.

We first characterized the NP suspensions before assessing their interference with a range of *in vitro* cytotoxicity assays, pro-inflammatory responses and oxidative stress detection methods. This strategy was used to determine which NP characteristics (composition, size, coatings, and agglomeration) are problematic for *in vitro* toxicity testing.

We observed important differences in NP interference with cytotoxicity assays depending on the type of NPs, their characteristics, and the test method. NR and MTT assays were problematic for TiO_2 and iron oxide NPs, which highly increased the OD reading for these dyes. This corroborates other studies on the interference of these types of NPs with formazan detection (Kroll et al. 2012; Griffiths et al. 2011), which can be attributed in part to the light-adsorbing properties of these NPs. However, our study showed that this phenomenon is more complex as some NPs displayed a greater interference with the NR assay than with MTT, both of which are measured at 550 nm. Furthermore the increase of the OD reading at 550 nm was even greater in the absence of the MTT reagent. In addition, the detection of the Griess reagent at this wavelength was only modified by the OC–Fe_3O_4 NPs but to a much greater extent than NR or MTT reagents. It has also been shown previously that NPs interfere with the MTT assay by adsorbing the tetrazolium salt (Wörle-Knirsch et al. 2006), or by releasing metal ions which modify the catalytic activity of the mitochondrial reductases (Kroll et al. 2009). Interestingly, when using the modified tetrazolium salt WST-1 the detection of formazan salt was only slightly modified by the presence of these NPs. This corroborates other studies showing no interference of TiO_2, SiO_2, quartz, MgO and ZnO NPs with the WST-1 assay (Wilhelmi et al. 2012). This could be due to the lower light-adsorbing properties of the NPs at 450nm, the detection wavelength of this dye. Furthermore, this water-soluble dye allowed the assessment of OD measurements in the cell culture supernatants after their transfer from the culture dishes to new plates. Ultracentrifugation can in this case be used to further reduce the particle load before analysis. We have demonstrated that this adaptation of the protocol helps to overcome the interference of cell-associated Fe_3O_4 NPs and to avoid false negative results. For the other assays, intensive washing steps may also improve the reliability of the results, if the NPs are not taken up by the cells. Gentle dissolution of the formazan in iPrOH/HCl without taking cell residues can also improve results.

Another cytotoxicity test, the LDH assay, did not display interference with the tested NPs. However, it has been reported for soluble NPs that metal ions could inactivate the LDH enzyme (Han et al. 2011). Furthermore, it has been shown that LDH could be adsorbed onto different NPs, especially TiO_2 NPs (Han et al. 2011; Wilhelmi et al. 2012). In our experimental design the NP suspensions containing LDH were not centrifuged, which otherwise could have led to the elimination of NP-adsorbed LDH. However, this adsorption capacity may be critical for NPs which have the property to alter the activity of enzymes as shown for carbon black NPs which can bind and inactivate N-acetyl-transferases by inducing conformational changes of the enzymes (Sanfins et al. 2011).

Cytotoxicity assays based on the measurements of proliferation or on cell counts have also been shown to be influenced by NPs. To the best of our knowledge, we demonstrate here for the first time that the presence of NPs could modify the radioactivity counts of ^{3}H-T using liquid scintillation. This result was observed independently by another partner of the NanoTest consortium (Jana Tulinska, personal communication). A possible explanation

for the apparent decrease of radioactivity counts can be the reduction of iron oxide NPs or adsorption of emitted electrons, thus diminishing the excitation of the scintillation fluid resulting in reduced cpm. On the other hand, optical quenching can also lead to diminished radioactivity measurements using liquid scintillation and interference of Fe_3O_4 NPs with ^{3}H-T detection can thus also be due to its optical properties. Automatic cell counting can also be problematic with NPs which tend to form large agglomerates. These agglomerates may lead to false cell counts by automatic systems and thus NPs without cells always need to be included as additional control and in case of interference cells should thus be analyzed manually. Furthermore, depending on the optical properties of the NPs, we show here that the agglomerates were counted as dead (U-Fe_3O_4) or alive (OC–Fe_3O_4) leading to underestimation or overestimation of cytotoxicity, respectively.

We have also shown that oxidative stress detection using fluorescent dyes can lead to false positive or false negative results, depending on the NP type. DCF as well as mBBr fluorescence signals were increased by TiO_2 NPs but decreased by the two iron oxide NPs used. Interestingly, it has also been shown by others that iron oxide NPs increase fluorimetric measurements of other probes such as calcein and 3′-(*p*-aminophenyl) fluorescein (APF) (Griffiths et al. 2011). However, we show here that quantification of fluorescence by flow cytometry using appropriate gating of the cell populations can account for these interferences as demonstrated for the PI staining of dead cells.

The study of pro-inflammatory responses using ELISA can also be critical due to adsorption of peptides, including cytokines, on NPs as demonstrated here for TiO_2, SiO_2 and Fe_3O_4 NPs. Interestingly, we observed an apparent increase in GM-CSF concentration in the presence of PLGA–PEO NPs. This may be due to the stabilization of the peptides, their protection from proteolysis or by avoiding the interaction of this cytokine with the plastic of the culture plates. Adsorption of cytokines, depending on the cytokine and NP type, has also been reported in other studies for a variety of NPs (Val et al. 2009; Xu et al. 2010; Turci et al. 2010). Our results show that the adsorption of cytokines did not only depend on the specific surface area of the NPs but also on their chemical nature as U-Fe_3O_4 NPs demonstrated higher adsorptions than Fl-25 SiO_2 NPs but had lower BET values. This cannot be explained solely by the negative charge of Fl-25 SiO_2 NPs as Fe_3O_4 NPs had even lower zeta potentials but the highest adsorption capacity, binding almost all cytokines present. These high adsorption capacities can also be critical for other assays as adsorption of dyes or substrates has been reported to interfere with cytotoxicity tests especially with single-walled carbon nanotubes which were shown to adsorb the MTT reagent (Wörle-Knirsch et al. 2006) or LDH (Han et al. 2011; Wilhelmi et al. 2012). Therefore, it is important to study the adsorption capacity of NPs before quantifying cytokine secretion induced by NPs, to avoid false negative or positive results using ELISA. Pretreatment of NPs for blocking their surface to avoid cytokine adsorption is unfortunately not possible as this will modify the surface of the NPs and thus their interaction with cells. In case of cytokine-adsorbing NPs, the induction of an inflammatory response can be investigated by measuring the production of cytokine mRNA by RT-qPCR. However, an increase of mRNA expression does not necessarily lead to an increase of protein secretion. The activation of cytokines is also regulated at the protein level such as IL-1beta maturation by the inflammasome complex. Another possibility is thus to study the basolateral cytokine secretion of cells cultured on semipermeable membranes, as only a few NPs could reach the basal compartment of such devices (see paper on transport of this special issue, Correia Carreira et al. 2015).

Table III. Summery of interferences observed with NPs and possible solutions.

Interference	Solution
Spectrophotometric measurements of NR	No further solution apart extensive washes
Spectrophotometric measurements of Griess reagent	No further solution apart extensive washes
Spectrophotometric measurements of formazan	Replacement by WST-1
Spectrophotometric measurements of WST-1	Transfer of supernatants to a new plate Ultracentrifugation of supernatants
Spectrofluorimetric measurements of H_2DCF-DA	Replacement by flow cytometric analysis
Spectrofluorimetric measurements of mBBr	Replacement by flow cytometric analysis
Flow cytometric measurements of PI, HE	Appropriate gating
LDH detection	Avoid centrifugation
^{3}H-thymidine radioactivity counts	Replacement by cell counting
Automatic cell counting	Replacement by manual cell counting
Cytokine quantification by ELISA	Detection in undernatants Replacement by RT-qPCR

Conclusions

Classic cytotoxicity testing strategies for chemicals need to be adapted by integrating NP-specific considerations. Interferences can be assay specific as well as NP specific. Metal oxides are more likely to interfere due to optical interferences, and certain particles due to their agglomeration or adsorption potentials. PLGA–PEO NPs have shown very few interference effects, since only a slight increase in OD readings of the MTT assay and in cytokine concentrations was observed.

It is therefore of crucial importance to test possible interference of all studied NPs with the foreseen methods prior to evaluating cellular responses to NPs. Scientists should report these results of interference tests along with toxicological data. In general, NPs should be eliminated from the analysis as much as possible in order to reduce the risk of interferences, for example, by extensive washing, ultracentrifugation, transferring supernatants or adaptation of gating. For some assays specific adaptations of the method procedure may be envisaged to avoid interferences but in some cases alternative methods should be considered (Table III). Visual examination of the cell cultures after their exposure to NPs is also an important element of the toxicological evaluation. However, this is not sufficient and additional verifications of NP interferences should be performed using the test systems, in parallel to the toxicity assays, in order to evaluate the impact of NPs on the test reliability.

A thorough physicochemical characterization of the NPs may already enable us to foresee putative interferences as particular NP properties could be problematic for specific techniques and assays (Figure 12). Interference with spectrophotometric and fluorimetric analyses depend on the optical properties of the NPs. The chemical composition, especially the surface chemistry, determines these properties and thus coatings could influence light absorption. Light scattering properties of, for example, TiO_2 NPs could also modify OD measurements as well as fluorimetric analyses. The agglomeration of NPs seems to play a smaller role in interference with spectrophotometric or fluorimetric analyses. TiO_2 and U-Fe_3O_4 NPs form large agglomerates in culture media, in contrast to OC–Fe_3O_4 NPs which show however the same level of interference. In contrast, other techniques such as flow cytometry or automatic cell counting may be problematic for agglomerating NPs. The surface

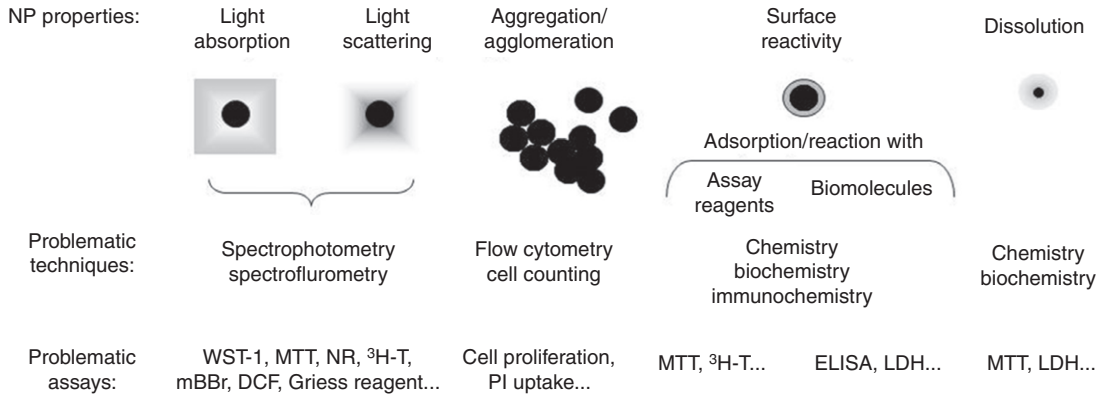

Figure 12. NP properties and interferences with assays.

reactivity of the NPs also determines their adsorption capacities and reactions with assay reagents or biomolecules. Ions dissolved from NPs can also interfere with, for example, enzyme-based assays by modulating their activities. The interference of NPs with toxicity methods that has been demonstrated may also occur with micrometric particles and should also be taken into consideration for their toxicity testing.

The physico-chemical analysis of NPs may thus allow the pre-selection of suitable assays. RT-qPCR or flow cytometry can be foreseen to replace some methods where interference is observed but these techniques are more time-consuming and cannot be used for high-throughput screenings of NPs. Testing strategies should thus take into consideration possible interferences for test reliability but also the feasibility of the replacement techniques.

Acknowledgements

This work was supported by NanoTEST project (Contract EC FP7 number 201335), EC FP7 QualityNano [INFRA-2010-1.131], Contract no: 214547-2, EC FP7 NANoREG, [NMP.2012.1.3-3], Contract no: 310584, and EC FP7 NanoTOES [PITN-GA-2010-264506]. The authors thankfully acknowledge Riccardo Cossi (Qi srl, Pomezia, Italy) for his valuable technical support, as well as Flavia Visin (University ''Ca' Foscari'' Venice) for ICP-OES analysis, respectively and to Imago Seine, imaging platform of Institut Jaques Monod (Nicole Boggetto) for flow cytometric analysis. The work undertaken by UH Bristol was carried out with the support of the Bristol Centre for Nanoscience and Quantum Information. Kevin Moreau provided technical help for work done at University Paris Diderot and work was supported by national funding from afsset (Contract N°EST-2008/1/49).Eric Rytting performed DLS analysis of SiO_2 NP samples.

Declaration of interest

The authors report no conflicts of interest. The authors alone are responsible for the content and writing of the paper.

References

Aitken RJ, Chaudhry MQ, Boxall AB, Hull M. 2006. Manufacture and use of nanomaterials: current status in the UK and global trends. Occup Med (Lond) 56:300–306.

Anders A, James B, Wim DJ, Philippe H, Thomas J, Mats-Olof M, et al. 2009. Risk assessment of products of nanotechnologies. European Commission, Directorate general for health and consumers, Public Health and Risk Assessment. 1–71. Available from: http://ec.europa.eu/health/ph_risk/committees/04_scenihr/docs/scenihr_o_023.pdf.

Barlow S, Chesson A, Collins JD, Flynn A, Hardy A, Jany K-D, et al. 2009. The potential risks arising from nanoscience and nanotechnologies on food and feed safety. EFSA J Eur Comm 958:1–39.

Brunauer S, Emmett P, Teller E. 1938. Adsorption of gases in multimolecular layers. J Am Chem Soc 60:10.

Correia Carreira S, Walker L, Paul K, Saunders M. 2015. The toxicity, transport and uptake of nanoparticles in the in vitro BeWo b30 placental cell barrier model used within NanoTEST. Nanotoxicology 9(S1):66–78.

Cedervall T, Lynch I, Lindman S, Berggård T, Thulin E, Nilsson H, et al. 2007. Understanding the nanoparticle-protein corona using methods to quantify exchange rates and affinities of proteins for nanoparticles. Proc Natl Acad Sci USA 104:2050–2055.

Damoiseaux R, George S, Li M, Pokhrel S, Ji Z, France B, et al. 2011. No time to lose–high throughput screening to assess nanomaterial safety. Nanoscale 3:1345–1360.

Doak SH, Griffiths SM, Manshian B, Singh N, Williams PM, Brown AP, et al. 2009. Confounding experimental considerations in nanogenotoxicology. Mutagenesis 24:285–293.

Griffiths SM, Singh N, Jenkins GJ, Williams PM, Orbaek AW, Barron AR, et al. 2011. Dextran coated ultrafine superparamagnetic iron oxide nanoparticles: compatibility with common fluorometric and colorimetric dyes. Anal Chem 83:3778–3785.

Halamoda Kenzaoui B, Chapuis Bernasconi C, Guney-Ayra S, Juillerat-Jeanneret L. 2012. Induction of oxidative stress, lysosome activation and autophagy by nanoparticles in human brain-derived endothelial cells. Biochem J 441:813–821.

Han X, Gelein R, Corson N, Wade-Mercer P, Jiang J, Biswas P, et al. 2011. Validation of an LDH assay for assessing nanoparticle toxicity. Toxicology 287:99–104.

Juillerat-Jeanneret L, Aguzzi A, Wiestler OD, Darekar P, Janzer RC. 1992. Dexamethasone selectively regulates the activity of enzymatic markers of cerebral endothelial cell lines. In Vitro Cell Dev Biol 28A: 537–543.

Kroll A, Pillukat MH, Hahn D, Schnekenburger J. 2009. Current in vitro methods in nanoparticle risk assessment: limitations and challenges. Eur J Pharm Biopharm 72:370–377.

Kroll A, Pillukat MH, Hahn D, Schnekenburger J. 2012. Interference of engineered nanoparticles with in vitro toxicity assays. Arch Toxicol 6: 1123–1136.

Lundqvist M, Sethson I, Jonsson BH. 2004. Protein adsorption onto silica nanoparticles: conformational changes depend on the particles' curvature and the protein stability. Langmuir 20:10639–10647.

Lundqvist M, Stigler J, Cedervall T, Berggård T, Flanagan MB, Lynch I, et al. 2011. The evolution of the protein corona around nanoparticles: a test study. ACS Nano 5:7503–7509.

Magdolenova Z, Bilaničová D, Pojana G, Fjellsbø LM, Hudecova A, Hasplova K, et al. 2012. Impact of agglomeration and different dispersions of titanium dioxide nanoparticles on the human related in vitro cytotoxicity and genotoxicity. J Environ Monit 14:455–464.

Maynard AD. 2007. Nanotechnology: the next big thing, or much ado about nothing? Ann Occup Hyg 51:1–12.

Monteiro-Riviere NA, Inman AO, Zhang LW. 2009. Limitations and relative utility of screening assays to assess engineered nanoparticle toxicity in a human cell line. Toxicol Appl Pharmacol 234:222–235.

Oberdörster G, Oberdörster E, Oberdörster J. 2005a. Nanotoxicology: an emerging discipline evolving from studies of ultrafine particles. Environ Health Perspect 113:823–839.

Oberdörster G, Maynard A, Donaldson K, Castranova V, Fitzpatrick J, Ausman K, IRFRSINTSW Group. 2005b. Principles for characterizing the potential human health effects from exposure to nanomaterials: elements of a screening strategy. Part Fibre Toxicol 2:8.

OECD. 2010. List of manufactured nanomaterials and list of endpoints for phase one of the sponsorship programme for the testing of manufactured nanomaterials: revision. OECD Environ Health Saf Publ Ser Saf Manufactured Nanomaterials 27:1–16.

Sanfins E, Dairou J, Hussain S, Busi F, Chaffotte AF, Rodrigues-Lima F, et al. 2011. Carbon black nanoparticles impair acetylation of aromatic amine carcinogens through inactivation of arylamine N-acetyltransferase enzymes. ACS Nano 5:4504–4511.

Stone V, Johnston H, Schins RP. 2009. Development of in vitro systems for nanotoxicology: methodological considerations. Crit Rev Toxicol 39:613–626.

Turci F, Ghibaudi E, Colonna M, Boscolo B, Fenoglio I, Fubini B. 2010. An integrated approach to the study of the interaction between proteins and nanoparticles. Langmuir 26:8336–8346.

Val S, Hussain S, Boland S, Hamel R, Baeza-Squiban A, Marano F. 2009. Carbon black and titanium dioxide nanoparticles induce pro-inflammatory responses in bronchial epithelial cells: need for multiparametric evaluation due to adsorption artifacts. Inhal Toxicol 21(Suppl 1):115–122.

Warheit DB, Sayes CM, Reed KL, Swain KA. 2008. Health effects related to nanoparticle exposures: environmental, health and safety considerations for assessing hazards and risks. Pharmacol Ther 120:35–42.

Wilhelmi V, Fischer U, van Berlo D, Schulze-Osthoff K, Schins RP, Albrecht C. 2012. Evaluation of apoptosis induced by nanoparticles and fine particles in RAW 264.7 macrophages: facts and artefacts. Toxicol In Vitro 26:323–334.

Wörle-Knirsch JM, Pulskamp K, Krug HF. 2006. Oops they did it again! Carbon nanotubes hoax scientists in viability assays. Nano Lett 6: 1261–1268.

Xu Z, Liu XW, Ma YS, Gao HW. 2010. Interaction of nano-TiO2 with lysozyme: insights into the enzyme toxicity of nanosized particles. Environ Sci Pollut Res Int 17:798–806.